Received: 19 October 2022 | Revised: 21 March 2023 | Accepted: 29 March 2023

DOI: 10.1002/cta.3620

ORIGINAL ARTICLE

WILEY

Very-low frequency capacitively coupled AC amplifier with a current feedback operational amplifier

Javier Beloso-Legarra[1,2] | **Carlos A. De La Cruz-Blas**[1,2] | **Alfonso Carlosena**[1,2] | **Maite Martincorena-Arraiza**[1,2]

[1]Department of Electrical, Electronic and Communications Engineering, Public University of Navarra, Pamplona, Spain

[2]Institute of Smart Cities, Public University of Navarra, Pamplona, Spain

Correspondence
Alfonso Carlosena, Department of Electrical, Electronic and Communications Engineering, Public University of Navarra, Campus de Arrosadia, E-31006 Pamplona, Spain.
Email: alfonso.carlosena@unavarra.es

Funding information
This work has been supported by the Spanish Research Agency, under grant AEI/FEDER PID2019-107258RB-C32, and by the Spanish Research Agency and the EU/PTR Next Generation Funds, under grant TED2021-131052B-C21, Agencia Estatal de Investigación, Ministerio de Ciencia e Innovación, Open access funding provided by Universidad Pública de Navarra.

Summary

In this paper, we propose the idea of using transimpedance amplifiers, in lieu of operational amplifiers (OAs) or transconductance amplifiers (OTAs) to design capacitively coupled AC amplifiers. The idea is demonstrated with a current feedback operational amplifier (CFOA) as an active element, which is actually an architecture consisting of voltage buffers and current copiers (mirrors). This last characteristic is further exploited to make the corner frequency of the AC amplifier tunable by means of bootstrapping low-valued resistors with the output buffer. It is particularly suited to achieve very-low corner frequencies as needed in applications such as bio- or seismic signals. The idea is demonstrated with simulations and experimental results with a discrete implementation.

KEYWORDS

AC coupled amplifier, bootstrapping, CFOA, low frequency

1 | INTRODUCTION

There are a number of sensors and transducers that provide a signal that contains DC, or very-low-frequency signals (i.e., baseline). Such low-frequency levels need to be removed to properly amplify the usable signal, thus requiring an AC amplifier, which basically exhibits a high-pass response with a zero at the origin and a pole at very low frequencies.[1] A classical solution is the so-called capacitive coupled AC amplifier,[2] whose basic structure is shown in Figure 1. The active element is a high-gain device, typically an operational amplifier (OA) or an operational transconductance amplifier, depending on the load at the output.

However, for signals with spectra in the range of few hertz, corner frequencies are so low that require time constants difficult to achieve with passive components of reasonable values. This is for instance the case of applications such as bio- or mechanical signals (seismology, structural health monitoring).[3] The problem aggravates for integrated implementations where particularly high-valued capacitors are not feasible, and high-valued resistors are not always available. To circumvent the problem, there are a number of solutions proposed in the literature at both architectural

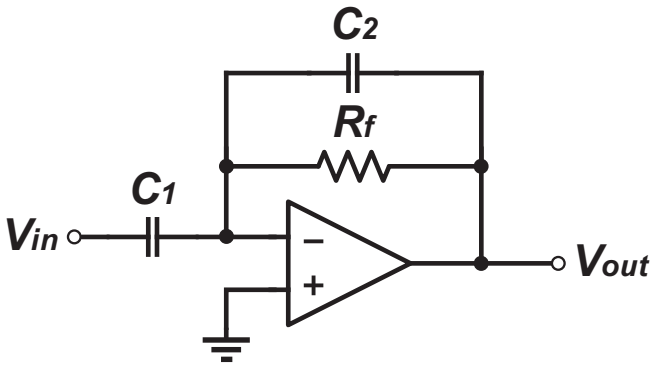

FIGURE 1 Capacitively coupled AC amplifier with a high gain voltage amplifier.

and circuit design levels. In most cases, active schemes are suggested that make use of amplification or bootstrapping mechanisms to increase by orders of magnitude the equivalent time constants of the circuit.

In this paper, we propose an alternative approach that makes use of transimpedance amplifiers as naturally suited to achieve large time constants with the conventional capacitive coupled AC amplifiers. The idea is exemplified and demonstrated with a commercial current feedback operational amplifier (CFOA), which is nothing but a particular implementation of a transimpedance amplifier. The scheme can be obviously implemented by different practical embodiments in both discrete and integrated forms.

Thus, the novelty of the paper consists of using transimpedance amplifiers and in particular the use of CFOAs. Actually, it is interesting to note that even though for most classical operational amplifier (OA) circuits a CFOA-based alternative has been proposed in the literature, this is, to the best of our knowledge, the first time a CFOA-based capacitive coupled AC amplifier is proposed. In fact, even the design of a Miller integrator has been questioned though demonstrated to work properly.[4] This is probably due to the misbelief that CFOAs cannot operate with capacitive feedback[5] or, as we will see, that the most remarkable advantage of CFOAs (gain-independent bandwidth) does not happen with this kind of feedback arrangement (but it is not needed).

In this paper, we also set the theoretical basis for the analysis and design of capacitively coupled AC amplifiers with CFOAs and by extension with transimpedance amplifiers. A comparison with their counterparts with other kinds of active devices would depend on the technology used, being out of the scope of this paper.

2 | PROPOSED CIRCUIT

The basic structure of a capacitively coupled AC amplifier is shown in Figure 1. Its transfer function, gain, and corner frequency are in the case of an infinite gain amplifier given by

$$\frac{V_{out}}{V_{in}} = -\frac{C_1 R_f s}{1 + C_2 R_f s} \qquad G = -\frac{C_1}{C_2} \qquad \omega_c = \frac{1}{R_f C_2} \tag{1}$$

where G is the DC gain and ω_c is the corner (high-pass) frequency. The block shadowed in Figure 1 can also be seen as a transimpedance amplifier, formed by the high-gain amplifier and feedback resistor, and the capacitive feedback divider formed by C_1 and C_2. Feedback resistor needs to be high enough to achieve a low corner frequency and is anyway needed to provide the bias current at the negative OA input. Alternatively, transimpedance can be readily provided by a CFOA, as shown in Figure 2A, where we exploit the fact that its transresistance is very high.

If we assume the model for a CFOA shown in Figure 2B, leaving apart for the moment the impedance of the output buffer R_o, circuit transfer function can be expressed as

$$\frac{V_{out}}{V_{in}} = -\frac{C_1}{C_2} \cdot \frac{1}{1 + \frac{R_x}{Z_T}\left(1 + \frac{C_1}{C_2}\right) + \frac{1}{Z_T C_2 s}} \tag{2}$$

where Z_T, that is, is the (grounded) transimpedance at gain node (also called compensation node), which is basically the parallel of a high-resistance R_T and a capacitance C_T. The resistance, high but with wide tolerances, provides high

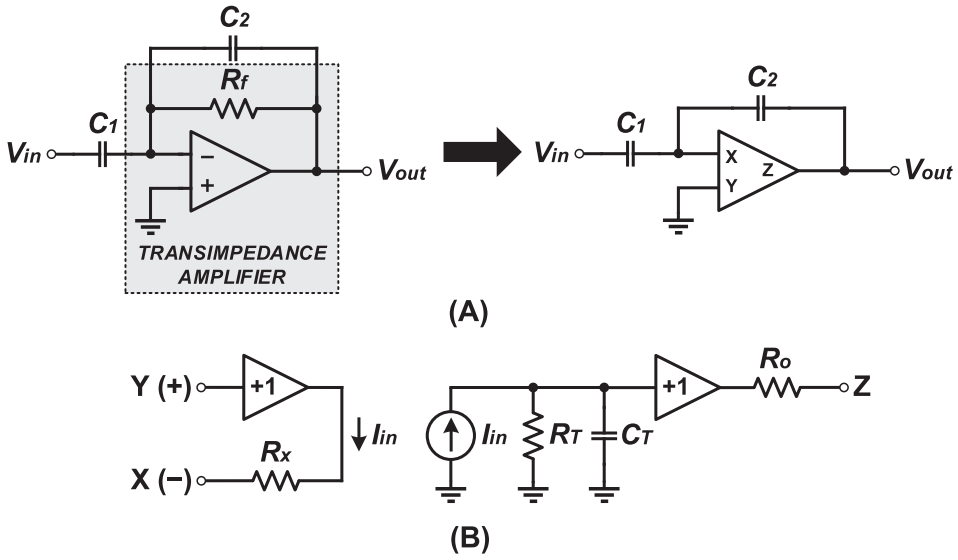

FIGURE 2 (A) AC coupled amplifier with transimpedance amplifier; (B) current feedback operational amplifier (CFOA) model.

transimpedance in the same way an OA provides a non-precise, very-high voltage gain. Feedback operation makes that for a finite output voltage, input current (and also current at gain node) is negligible mimicking the operation of a conventional OA, where input currents are negligible but due to the high impedance. Capacitance C_T is introduced to set the system bandwidth in combination with the feedback resistance, connecting the CFOA output and its negative (x) input. In this way, bandwidth can be made independent of gain by fixing feedback resistor. However, as we will see, this is not the case for a capacitively coupled AC amplifier.

Approximating Expression (2) for low frequencies, where the effect of capacitance C_T can be neglected, the high-pass corner frequency, ω_{ch}, can be calculated as

$$\omega_{ch} = \frac{1}{R_T C_2} \cdot \frac{1}{1 + \frac{R_x}{R_T}\left(1 + \frac{C_1}{C_2}\right)} \tag{3}$$

Since $R_x \ll R_T$, corner frequency is basically determined by the product $R_T C_2$. This does not come as a surprise since R_T is the transimpedance of the CFOA, in the same way that R_f is the transimpedance of circuit in Figure 1A that results in Expression (1). As we explained before, this value, in the range of MΩ, is subjected to wide tolerances in a conventional CFOA, since it depends on current mirror output impedance and buffer input impedance at compensation node. Transresistance R_T, apart from fabrication tolerances, is also dependent on biasing voltages and temperatures. If we consider the case of the commercial CFOA model AD 844 (which will be used later in our simulations and measurements), its transresistance may vary from 1.4 to 4 MΩ (for the extreme conditions in supply voltage and temperature). In consequence, the corner frequency would vary in a range 1:3, if no bootstrapping were used. Maximum transresistance, that is, minimum corner frequency, results for high temperature and biasing voltages. Therefore, to achieve a controllable corner frequency, a tuning mechanism should be provided, as we explain below.

A way to do this is by means of the so-called bootstrapping[6] that has been used in the past in different ways. Generally speaking, the technique refers to a partial positive feedback that forces two nodes to have very close voltages and/or reduce the current between them. It has been used in AC amplifiers with OAs and OTAs[2,7,8] and also with current conveyors.[9] Here, we make use of the CFOA output buffer and a resistive T-network to set the high resistance at compensation node. The technique was originally proposed in Note et al.[10] as a mechanism to simulate a high resistance and to assure a proper bias current for a buffer when this is disconnected from the input. More recently a similar embodiment has been used to boost the input impedance of an amplifier for dry ECG electrodes.[11] This is schematically shown in Figure 3. Input impedance at the output buffer, not counting R_T, can be calculated as

$$R_B = R_1\left(1+\frac{R_2}{R_1}+\frac{R_2}{R_3}\right) \tag{4}$$

which can be made arbitrarily high by playing with resistor ratios. Therefore, transimpedance, which is the parallel effect of R_B and R_T, can be made controllable and tunable.

We should remark at this point that a transimpedance amplifier, as proposed for this application, can be implemented by making use of only voltage buffers and current copiers as active elements, which are the basic building blocks of a conventional architecture of a CFOA. Depending on the application, the designed AC amplifier can be optimized by only resorting to the design of voltage or current copiers. In particular, the design can be focused to achieve a high resistance R_T since this value sets the limit for the minimum achievable corner frequency.

Though CFOAs were initially proposed to work in conditions similar to OAs with two input terminals and a single output,[12,13] the availability of the compensation node adds flexibility to the topology, allowing alternative and novel applications.[14–17] Our application is one such. Unfortunately, the number of commercial CFOA devices that have the compensation node externally available is scarce, the model AD844 being a remarkable exception.[18]

If we analyze now the behavior at high frequencies of the AC amplifier, then the low-pass frequency ω_{cl} can be calculated from Expression (2) as

$$\omega_{cl} = \frac{1}{R_x C_T}\cdot\frac{\left(1+\frac{C_T}{C_2}\right)}{\left(1+\frac{C_1}{C_2}\right)} \tag{5}$$

In a first interpretation, we could conclude that bandwidth is very high, since R_x and C_T are very low. This value reduces however proportionally to circuit gain C_1/C_2. This result contradicts the main rationale behind the use of CFOA, where constant bandwidth versus gain is pursued. In our application what is however relevant is the high-transresistance offered by the CFOA since we are designing an application intended for low-frequency signals, and bandwidth will have to be reduced anyway. We will come back to this issue in the next section, since high-frequency behavior strongly depends on output impedance at the output buffer, R_0.

3 | SECOND-ORDER ANALYSIS

The analysis presented in the previous section has allowed to show the main features of the proposed circuit in terms of low-frequency behavior and tunability. However, high-frequency behavior requires a finer analysis by considering the effect of output impedance R_0; see Figure 2B. In what follows, we will assume that R_0 accounts also for the effect of the T network (which reduces the buffer output impedance), and that in the same way R_T includes the effect of both CFOA transresistance at compensation node and R_B.

According to the complete model in Figure 2B, transfer function can be calculated as

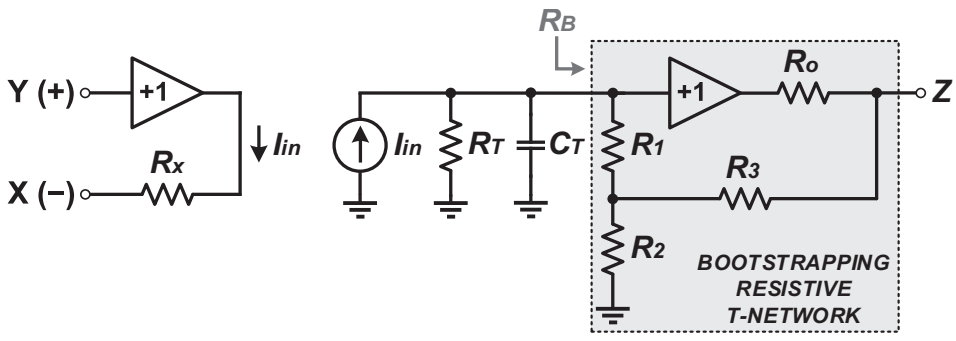

FIGURE 3 Bootstrapping of the output buffer with a resistive T-network.

$$\frac{V_{out}}{V_{in}}=\frac{-C_1R_Ts+C_1C_2R_xR_0s^2+C_1C_2C_TR_xR_0R_Ts^3}{1+(C_1R_x+C_2(R_x+R_0+R_T)+C_TR_T)s+(C_1C_2R_xR_0+C_TR_T(C_1R_x+C_2(R_x+R_0)))s^2+C_1C_2C_TR_xR_0R_Ts^3} \tag{6}$$

In a first step, denominator can be simplified by just considering that $R_T \gg (R_o, R_x)$ and $C_T \ll (C_1, C_2)$ yielding the following approximation:

$$\frac{V_{out}}{V_{in}} \approx -\frac{C_1R_Ts-C_1C_2R_xR_0s^2-C_1C_2C_TR_xR_0R_Ts^3}{1+C_2R_Ts+C_TR_T(C_1R_x+C_2(R_x+R_0))s^2+C_1C_2C_TR_xR_0R_Ts^3} \tag{7}$$

The above expression can be factorized to identify the low- and high-frequency responses as follows:

$$\frac{V_{out}}{V_{in}} \approx -\frac{C_1R_Ts}{1+C_2R_Ts}\cdot\frac{1-C_2\frac{R_xR_0}{R_T}s-C_2C_TR_xR_0s^2}{1+\frac{C_TR_T(C_1R_x+C_2(R_x+R_0))}{1+C_2R_Ts}s^2+\frac{C_1C_2C_TR_xR_0R_T}{1+C_2R_Ts}s^3} \tag{8}$$

The left factor corresponds to the low-frequency response where gain $-C_1/C_2$ and high-pass corner frequency $1/(R_TC_2)$ are easily identified. Right factor can be further simplified taking into account that $|C_2R_Ts| \gg 1$, leading to a more manageable expression:

$$\frac{V_{out}}{V_{in}} \approx -\frac{C_1R_Ts}{1+C_2R_Ts}\cdot\frac{1-C_2\frac{R_xR_0}{R_T}s-C_2C_TR_xR_0s^2}{1+\left(C_T\frac{C_1}{C_2}R_x+C_T(R_x+R_0)\right)s+C_1C_TR_xR_0s^2} \tag{9}$$

Numerator contains two high-frequency zeroes that can be calculated as

$$z_{1,2}=-\frac{1}{2\,C_TR_T}\mp\frac{\sqrt{{C_2}^2{R_0}^2\left(\frac{{R_x}^2}{{R_T}^2}+4\frac{C_T}{C_2}\frac{R_x}{R_0}\right)}}{2\,C_2C_TR_xR_0} \tag{10}$$

If $({R_x}^2/{R_T}^2) \ll (C_T/C_2)$, which is the case in practical situations, above expression becomes

$$z_{1,2} \approx -\frac{1}{2\,C_TR_T}\mp\frac{1}{\sqrt{C_2C_TR_xR_0}} \tag{11}$$

That is to say, two real zeroes, one on each side of the s-plane with very close values, are given by

$$z_{1,2} \approx \mp\frac{1}{\sqrt{C_2C_TR_xR_0}} \tag{12}$$

Regarding the poles, if we consider that circuit gain C_1/C_2 is high, the first-order term in denominator can be approximated by $(C_TC_1)/(C_2R_x)$. Then, we obtain two poles of the form:

$$p_{1,2} \approx -\frac{1}{2\,C_2R_o}\left(1\pm\sqrt{\left(1-4\frac{{C_2}^2}{C_TC_1}\frac{R_o}{R_x}\right)}\right) \tag{13}$$

For a given gain, these two poles depend mainly on C_2. As it increases, not only the pole values reduce, and thus bandwidth, but they may become complex conjugate, bringing along the corresponding peaking in the frequency response and eventually instability. Note that this result differs greatly from the bandwidth estimation given by the first-order approximation in Expression (5). To make both poles real and avoid the aforementioned peaking, capacitor C_T can be used to compensate and control the damping factor. Once fixed C_1 and C_2 as design variables, and since R_x and R_o depend on CFOA characteristics, the following condition should be satisfied:

$$1-4\frac{C_2{}^2}{C_T C_1}\frac{R_o}{R_x}\geq 0 \tag{14}$$

which leads to a minimum compensation capacitor of

$$C_T \geq 4\frac{C_2{}^2}{C_1}\frac{R_o}{R_x} \tag{15}$$

The condition is easy to be fulfilled for high gains but may become critical for low gains that would require unacceptable high C_T. Moreover, for high C_T values, the closed-loop gain may decrease, according to (2). This is especially critical for very large compensation values in the order of C_1 and C_2. If condition given by (15) is not fulfilled, it does not mean however that the circuit will become unstable. This will be analyzed in more detail in the next paragraphs.

Under these conditions, that is, high-frequency response dominated by C_T, Expression (5) can be considered a good approximation, and we have a kind of a constant "gain-bandwidth product." From Expression (2), we can also approximate the mid-band gain, which results in the following expression:

$$G=-\frac{C_1}{C_2}\cdot\frac{1}{\left(1+\frac{C_T}{C_2}\right)} \tag{16}$$

This means that the compensation with C_T brings along the undesirable effect of reducing gain, which can be noticeable when C_T is in the order of C_2. A simpler alternative consists of adding a resistor R_{in} in series with C_1, setting a pole at $1/(R_{in}C_1)$.

In order to check to which extent the approximations for poles and zeroes are correct, we have carried out a numerical analysis of the transfer function and the approximated expressions for poles and zeroes. Figure 4 compares a plot of the transfer function in Expression (6) with the transfer function that would result of the combination of poles and zeroes in Expressions (3), (5), (11), and (13). Both curves are indistinguishable, demonstrating the validity of pole and zero estimations. The values used for the passive components are those in Table 1, which will be the same for measurements. In the case of C_T, it comprises the internal CFOA capacitance of 4.5 pF, as well as the breadboard parasitic capacitance, which is approximately 15.5 pF and an externally connected capacitance of 10 pF. In this way, the condition given by Equation (15) is easily met. We note that the internal parameters of the CFOA correspond to those extracted from the datasheet of the AD844 CFOA, which will be used for the experimental measurements.

The model considered so far, given by Equation (5), and its simplified approximation, given by the poles and zeroes calculated, do not take into account other effects such as frequency dependence of output impedances, or additional poles in the CFOA response. Therefore, we have compared our model with a more precise macromodel made available by the manufacturer. To this end, we have included in Figure 4 the frequency response simulated by spice under the same conditions. Figure 4A corresponds to the low-frequency response where the three curves are indistinguishable. In Figure 4B, we show that the high-frequency response is also the same for the complete and simplified model, where the simulation only differs significantly at frequencies close to the CFOA bandwidth.

If we fit the simulated frequency response to a third-order model, the relative differences of the poles and zeroes estimated with respect to those calculated by Equations (3) and (13) are 1.2% for the low-frequency pole (corner frequency) and 6% and 14% for the high-frequency poles located at 1.13 and 11.06 MHz. The conclusion is that the simplified model represents a good balance between accuracy and simplicity in the equations to allow an easy design.

We have also verified that a fit to a fourth-order model from the simulated response gives more accurate results, but this is achieved at the expense of losing the connection between circuit parameters and poles and zeroes (or characteristic frequencies).

To have a finer grasp of the stability conditions given by Equation (15), we can calculate and estimate the phase margin of the circuit. First of all, manipulating transfer function given by Equation (6) with the method proposed in Ochoa,[19] we obtain the following loop-gain (LG) transfer function:

$$LG=-\left(\frac{sC_2}{1+C_T R_T s}\right)\left(\frac{1}{1+(C_1+C_2)R_x s}\right)\left(\frac{1}{1+C_2 R_o s}\right)(R_T-C_2 R_x R_o(1+C_T R_T s)s) \tag{17}$$

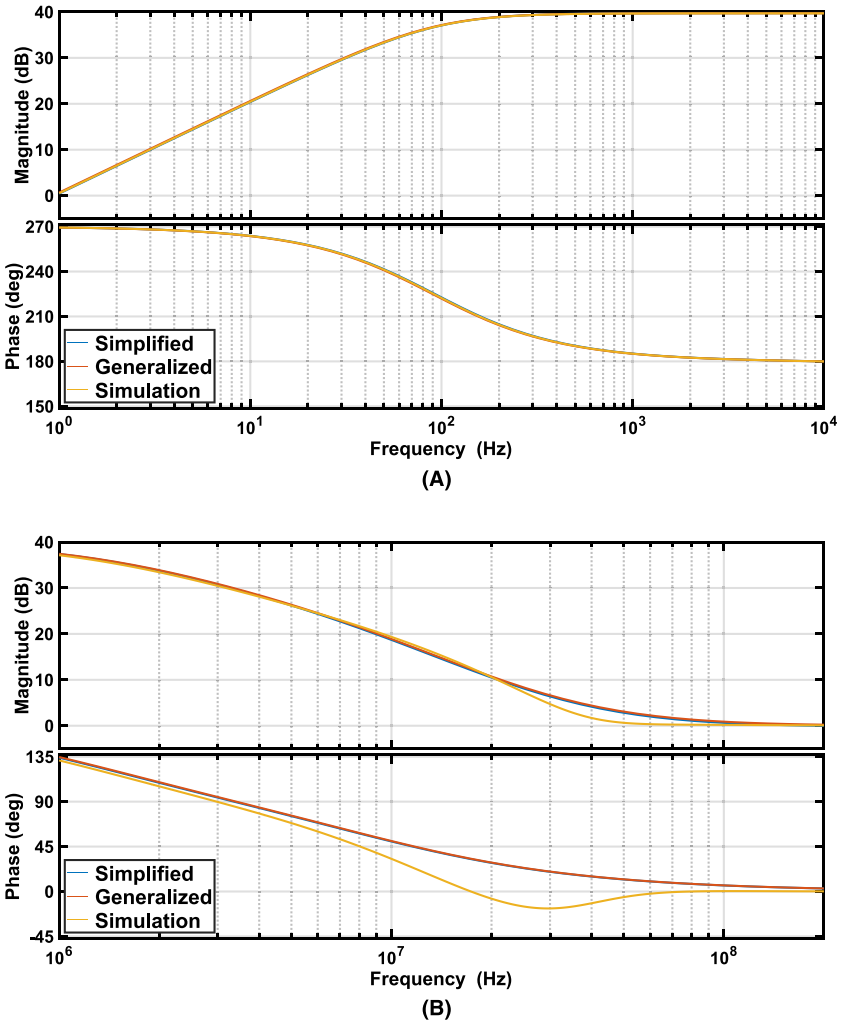

FIGURE 4 Comparison of transfer functions. (A) Low- and (B) high-frequency response. [Colour figure can be viewed at wileyonlinelibrary.com]

TABLE 1 Design variables.

Parameter	Value
C_1	10 nF |33 nF|100 nF
C_2	1 nF
C_T	30 pF
R_1	10 kΩ
R_2	10 kΩ
R_3	10 Ω |100 Ω|1 kΩ|10 kΩ
R_T	3 MΩ
R_x	50 Ω
R_o	15 Ω

To develop the phase margin expression, Equation (17) is simplified by considering only the mid-band frequency range that contains the two high-frequency poles of (13) and constants. The resulting expression is

$$LG \approx -\frac{C_2}{C_T}\cdot\left(\frac{1}{1+(C_1+C_2)R_x s}\right)\left(\frac{1}{1+C_2R_o s}\right) = -A\left(\frac{1}{1+s/\omega_{p1}}\right)\left(\frac{1}{1+s/\omega_{p2}}\right) \tag{18}$$

where $A = C_2/C_T$, $\omega_{p1} = 1/(C_1+C_2)R_x$, and $\omega_{p2} = 1/C_2R_o$ with $\omega_{p1} < \omega_{p2}$. The distance between both poles is a measure of the stability, and it is obviously higher for higher gains. If these two poles are well separated, we can use the phase margin expression[20] $PM = 90^\circ - tg^{-1}(A\omega_{p1}/\omega_{p2})$, which results in the following expression:

$$PM = 90^\circ - tg^{-1}\left(\frac{{C_2}^2}{C_T(C_1+C_2)}\frac{R_o}{R_x}\right) \tag{19}$$

which, for a given gain, C_2, and a desired PM, leads to a minimum value for the compensation capacitor of

$$C_T = \frac{1}{tg(90^\circ - PM)}\frac{{C_2}^2}{(C_1+C_2)}\frac{R_o}{R_x} \tag{20}$$

Notice the similarity of the above expression to Equation (15) with the addition of the phase margin as a design variable. From the comparison, we can make some numerical basic estimations to see that the condition for real poles (exp (15)) at a gain of 40 dB corresponds to a phase margin of 75°. For a gain of 20 dB, the gain margin would be 65°, but requiring of course a larger compensation capacitor.

The complete loop gain transfer function is plotted in Figure 5 for the parameters in Table 1 ($R_3 = 10\,\Omega$) and several gains. The resulting phase margins are 54.7°, 76.0°, and 86.3° for gains of 20, 30, and 40 dB, respectively. Using Equation (19), the phase margins are 47.7°, 73.6°, and 84.3° for the same gains. All these analyses show that Equation (19) is a good approximation to estimate phase margin.

According to the analysis carried out so far, we deem interesting to summarize the steps that should be taken to design an AC amplifier with a CFOA:

1. Determine the desired minimum corner frequency $\omega_{ch} \rightarrow$ calculate $C_2 = 1/(R_T \cdot \omega_{ch})$ with R_T being the CFOA transimpedance.
2. Determine the desired gain $G \rightarrow$ calculate $C_1 = G \cdot C_2$.
3. Set, if needed, a compensation capacitor C_T according to Equation (15). If the resulting value is higher than capacitance at gain node of the CFOA, this is not required.
4. If C_T is too high, say, $C_2/C_T < 100$, $\rightarrow$ recalculate C_1 using Expression (16).
5. In case ω_{ch} needs to be increased $\rightarrow$,

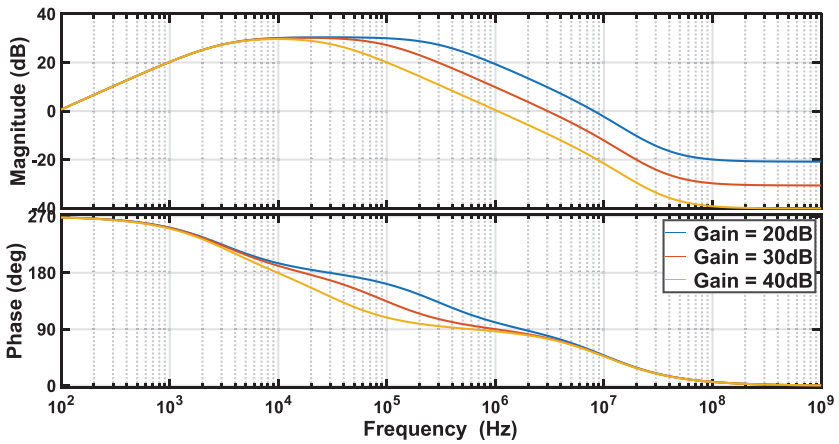

FIGURE 5 Magnitude and phase response of the loop gain. [Colour figure can be viewed at wileyonlinelibrary.com]

a. Go to step (1) and increase C_2, or
b. Introduce R_T by bootstrapping so that $C_2 = 1/((R_T \parallel R_B) \cdot \omega_{ch})$ where R_B is given by Equation (4).

Option b. gives a better (lower) sensitivity of the corner frequency with respect to process, bias, and temperature variations.

We recall that step (3) gives a safety margin for stability, since it assures real high-frequency poles. A lower capacitance will also result in a stable circuit, but exhibiting peaking in the frequency response and a longer transient. Alternatively, Expression (20) can be used to set C_T with a prescribed phase margin.

4 | EXPERIMENTAL ANALYSIS

The experimental results shown below have been obtained by making use of the AD844, which is the commercial CFOA that provides access to the gain node. Its most relevant parameters are included in Table 1. They correspond to biasing voltages of ±15 V. These are typical characteristics, which have wide deviations depending on temperature and biasing voltages, particularly for transimpedance and output impedance, as we explained in a previous section. At the end of the section, we will show some experimental results with different biasing voltages.

The experimental setup is shown in Figure 6. It simply consists of an Arbitrary Wave Generator Agilent 33522A, which is parametrized to generate sinusoidal sweeps in the desired frequency ranges. Given the low frequencies to be measured, sweep duration can be up to tenths of seconds. The circuit under test is excited with such signal and both input and output are acquired by a Tektronix MSO44 Scope in Spectrum View © mode, which allows for the calculation of input and output spectra, and thus frequency response.

We will first show the behavior at low frequencies for different gain and corner frequency values. This is shown in Figure 7. Starting from the minimum achievable frequency, which is set by the product $R_T C_2$, it can be increased by the above bootstrapping mechanism described previously. In the measurements, C_1 is varied to obtain different gains (20, 30, and 40 dB), C_2 is fixed to 1 nF and resistors used in the T-network are those shown in Table 1. The equivalent R_T values are (including the 3 MΩ internal CFOA transresistance) 1.7, 890, 120, and 30 kΩ for R_3 equal to 10 Ω, 100 Ω, 1 kΩ and 10 kΩ, respectively.

Experimental values for the corner frequencies agree well with those theoretically predicted though in the case of the lower frequencies they become less predictable since they are mainly determined by the transresistance at compensation node.

As we mentioned earlier in the paper, the transresistance limits both closed-loop accuracy as well as the minimum high-pass cut-off frequency. Since it depends on the output resistance of the input current-conveyor, which in turn depends on the output transistor resistances that are non-linear devices, it varies with both supply voltage and temperature. In Figure 8, we show the effect of the high-pass cut-off frequency for $C_1 = 100$ nF, $C_2 = 1$ nF, and $R_3 = 10$ Ω under several supply voltage variations (±5, ±10, and ±15 V). Such variations drastically reduce as the bootstrapping resistance, R_B, given by Equation (4), diminishes, making corner frequency less dependent on the device transimpedance.

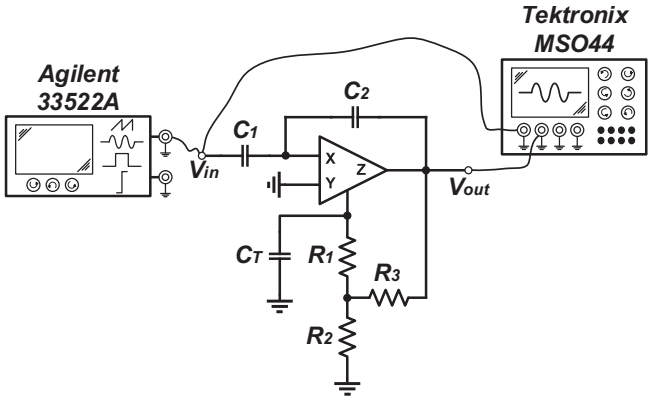

FIGURE 6 Experimental setup.

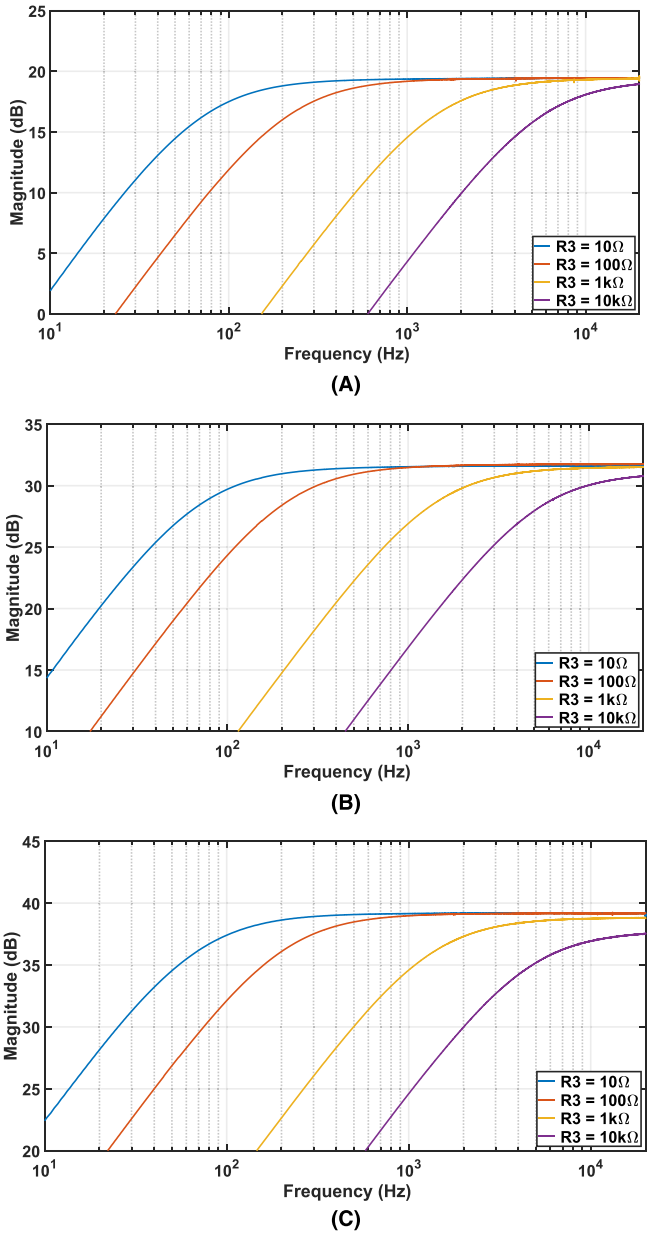

FIGURE 7 Low-frequency behavior for different gains and bootstrapping values. [Colour figure can be viewed at wileyonlinelibrary.com]

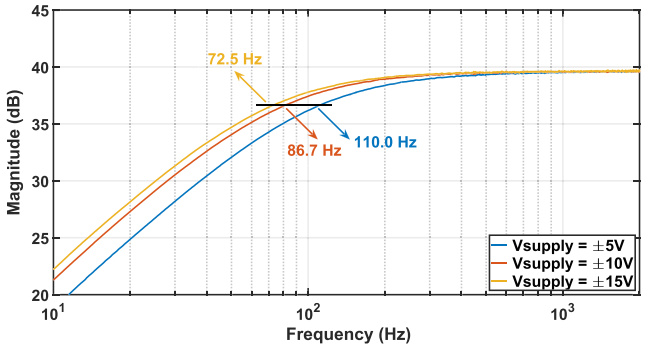

FIGURE 8 Corner frequency variations depending on biasing voltages. [Colour figure can be viewed at wileyonlinelibrary.com]

Regarding high-frequency behavior, the circuit has been measured for the same gains. Passive components have been chosen so that, according to Expression (13), peaking is evident for low gains and is diminished for higher ones, where phase margin is improved accordingly. An external capacitor of 10 pF has been added to the compensation node to render an equivalent capacitance of 30 pF and avoid instability. Measurements in Figure 9, for a fixed R_3 of 10 Ω, show a peaking around 10 dB for a gain of 20 dB, almost vanishing for 40 dB. High-frequency zeroes do not show up in the measurement range, since they are theoretically located at approximately 33.5 MHz.

To see how compensation capacitance C_T at gain node affects the response, we have artificially increased its value up to 1 nF. Results for several values are shown in Figure 10 where gain is 40 dB and R_3 is 10 Ω. As predicted in Expression (5), a dominant pole with a 20 dB/decade roll-off shows up at around $1/R_xC_T$. From measurements, and assuming this approximation is correct, R_x can be estimated in 70 Ω, which is slightly higher than the nominal value given in the datasheet. Measured frequency response also shows a mid-band gain reduction that can be explained by Expression (16). If C_2 is constant, such reduction does not depend on gain. Another observable effect is the presence of a zero compensating the pole, which can be explained by the movement of the high-frequency zero due to the increase in C_T, according to Expression (11).

In Figure 11, we can see the effect of introducing a resistor R_{in} in series with C_1 to reduce bandwidth and eventually improve stability. The result is similar to compensating with C_T but without the negative effect of gain reduction at mid frequencies. The effect of the zero is not present in this case.

Finally, we have compared the performance of a capacitively coupled AC amplifier implemented by an OA and a CFOA. Considering that the CFOA model AD844 exhibits a bandwidth between 30 and 60 MHz depending on the feedback conditions, to make a fair comparison we have selected the OA AD826 that shares the same bipolar technology and a similar frequency range in order. The feedback resistor R_f in the OA-based AC amplifier, shown in Figure 1, is adjusted to the same value as the equivalent resistance of the T-network used for bootstrapping, R_B in the CFOA based that shown in Figure 6. The feedback capacitors are obviously the same. Under these conditions, both gain and corner (high-pass) frequency of the two amplifiers should be the same.

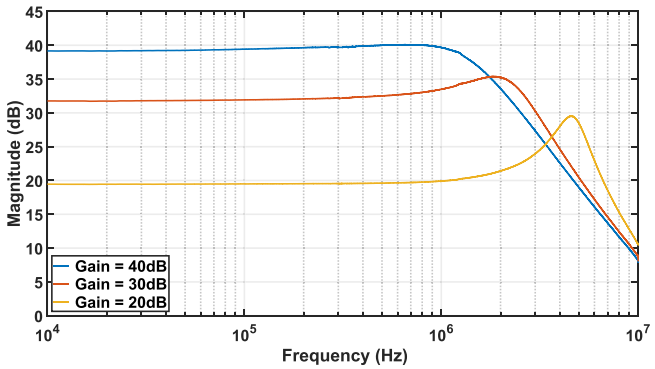

FIGURE 9 High-frequency behavior for different gains. [Colour figure can be viewed at wileyonlinelibrary.com]

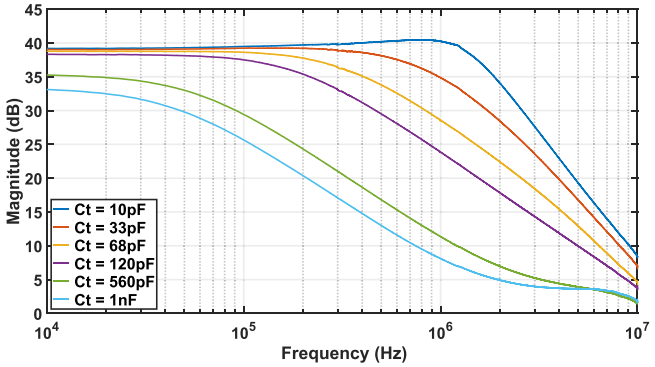

FIGURE 10 Effect of C_T in the high-frequency behavior. [Colour figure can be viewed at wileyonlinelibrary.com]

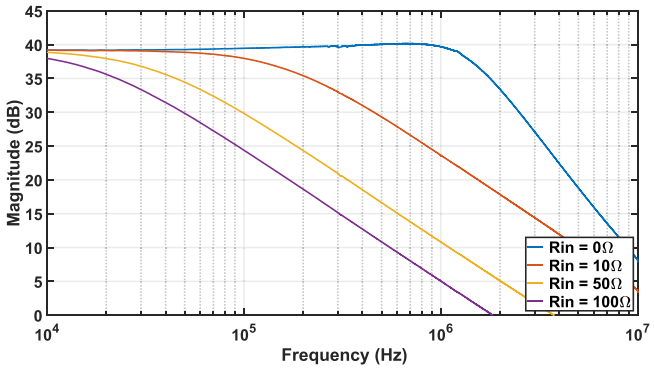

FIGURE 11 Effect of R_{in} in the high-frequency behavior. [Colour figure can be viewed at wileyonlinelibrary.com]

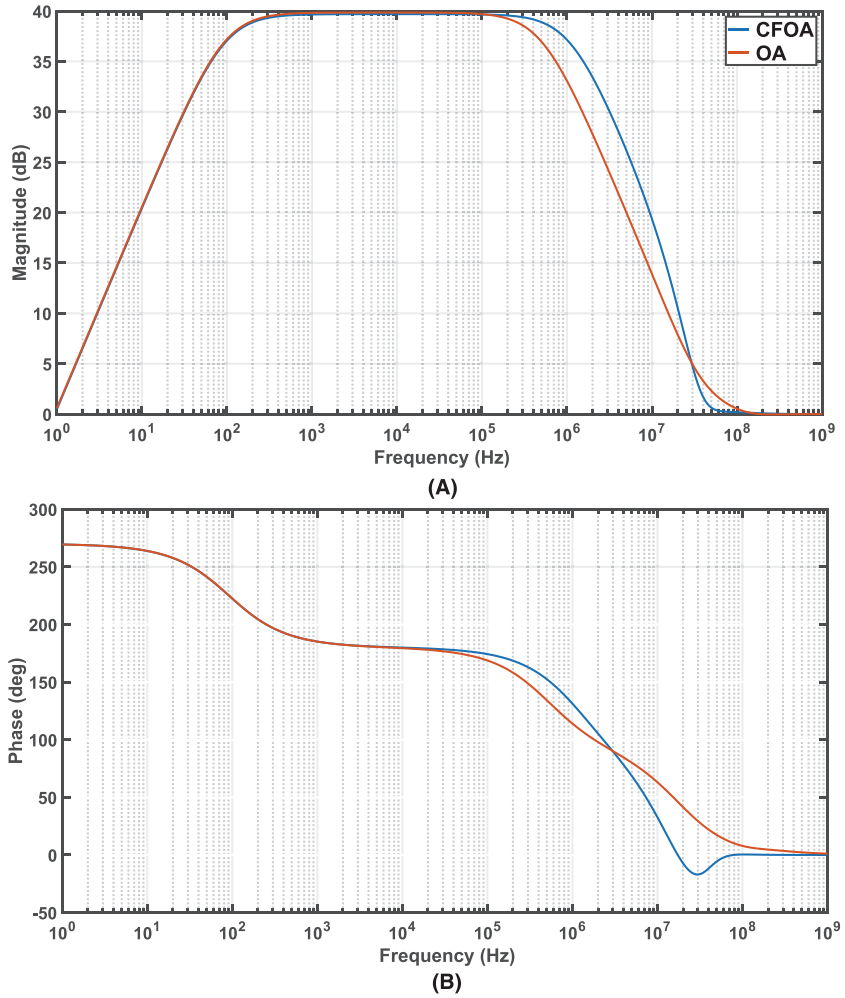

FIGURE 12 Comparison of a capacitively coupled AC amplifier based on CFOA and OA. Frequency response in terms of (A) magnitude and (B) phase. [Colour figure can be viewed at wileyonlinelibrary.com]

The analysis of the OA-based topology can be found elsewhere, and it is evident that what differentiates it with respect to the CFOA based, introduced in this paper, is the high-frequency behavior. In the case of the OA, high-frequency behavior mainly depends on the OA gain-bandwidth product, whereas we have shown that in the case of the CFOA, it mainly depends on the buffers' output resistance. This reflects in the simulations shown in Figure 12. As expected, low-frequency corner frequencies and gains are the same, whereas high-frequency behaviors show different

patterns because of the different pole-zero locations. Bandwidth is higher for the CFOA, but this cannot be seen as a relevant advantage since for most applications, bandwidth has to be limited anyway.

Advantages and disadvantages of one or the other topology should be analyzed in the light of a specific application, and for a given technology, and thus, general rules cannot be given. We do not claim the superiority of CFOA-based amplifiers but have just opened in our paper the possibility to design capacitively coupled AC amplifiers, with transimpedance amplifiers, and CFOAs in particular.

5 | CONCLUSIONS

In this paper, we have demonstrated a capacitively coupled AC amplifier using a single CFOA as an active device. Contrary to the common belief, we have shown that a CFOA can work with a purely capacitive feedback without the need of resorting to extraneous passive values, or forced compensation schemes. The circuit has been modeled, and its performance can be easily explained in terms of simplified expressions for high-frequency poles and zeroes. A closed-form expression to estimate the phase margin has been also obtained.

The circuit has been experimentally demonstrated with the commercially available AD844 CFOA, which makes the gain node externally available. Unfortunately, this feature is not present in most commercial CFOAs. The circuit renders a corner frequency in the range of a few hertz when gain node is not used, but the frequency can be reduced in a controllable way by bootstrapping its output buffer.

The analysis carried out paves the way to application-oriented capacitively coupled AC amplifiers, where a CFOA (or in general a transimpedance amplifier) is the active element. Though commercially available CFOAs pose some limitations, the design can be optimized for specific applications if a fully integrated implementation is available.

DATA AVAILABILITY STATEMENT

Data sharing not applicable to this article as no datasets were generated or analysed during the current study.

ORCID

Javier Beloso-Legarra https://orcid.org/0000-0002-0490-9575
Maite Martincorena-Arraiza https://orcid.org/0000-0001-7932-5534

REFERENCES

1. Casas O, Spinelli EM, Pallàs-Areny R. Fully differential AC-coupling networks: a comparative study. *IEEE Trans Instrum Meas*. 2009; 58(1):94-98. doi:10.1109/TIM.2008.927200
2. Martincorena-Arraiza M, Carlosena A, De La Cruz-Blas CA, Beloso-Legarra J, Lopez-Martin A. A family of AC amplifiers for ultra-low frequency operation. *Int J Circuit Theory Appl*. 2021;49(10):3317-3327. doi:10.1002/cta.3122
3. Harrison RR. The design of integrated circuits to observe brain activity. *Proc IEEE*. 2008;96(7):1203-1216. doi:10.1109/JPROC.2008.922581
4. Toumazou C, Mahattanakul J. A theoretical study of the stability of high frequency current feedback Op-Amp integrators. *IEEE Trans Circuits Syst I: Fund Theory Appl*. 1996;43(1):2-12.
5. Senani R, Bhaskar DR, Singh AK, Singh VK. *Current Feedback Operational Amplifiers and Their Applications*. Springer US; 2013. doi:10.1007/978-1-4614-5188-4
6. Seevinck E, Member S, Plessis M. Active-bootstrapped gain-enhancement technique for low-voltage circuits. *IEEE Trans Circuits Syst II: Analog Digital Signal Process*. 1998;45(9):1250-1254. doi:10.1109/82.718592
7. Martincorena-Arraiza M, Carlosena A, De La Cruz-Blas CA, Lopez-Martin A. AC coupled amplifier with a resistance multiplier technique for ultra-low frequency operation. *AEU-Int J Electron C*. 2022;149:154176. doi:10.1016/j.aeue.2022.154176
8. Aminzadeh H, Dashti A. Hybrid cascode compensation with current amplifiers for nano-scale three-stage amplifiers driving heavy capacitive loads. *Analog Integr Circuits Signal Process*. 2015;83(3):331-341. doi:10.1007/s10470-015-0522-2
9. Stornelli V, Ferri G. A single current conveyor-based low voltage low power bootstrap circuit for ElectroCardioGraphy and ElectroEncephaloGraphy acquisition systems. *Analog Integr Circuits Signal Process*. 2014;79(1):171-175. doi:10.1007/s10470-013-0252-2
10. Note A, Impedance H, Amps O, Number L. "*Impedance Op Amps AN-241*".
11. Maji S, Burke MJ. A bootstrapping technique to boost input impedance of ECG recording amplifiers. In: *Conference Record—IEEE Instrumentation and Measurement Technology Conference*; 2022. doi:10.1109/I2MTC48687.2022.9806565
12. Nelson D, Evans S. "*Application Note 3001, A New Approach to Op-Amp Design*," 1985.
13. Franco S. Analytical foundations of the current-feedback amplifiers. In: *IEEE International Symposium on Circuits and Systems*; 1993: 1050-1053. doi:10.1109/ISCAS.1993.393914

14. Senani R, Bhaskar DR, Kumar P. Two-CFOA-grounded-capacitor first-order all-pass filter configurations with ideally infinite input impedance. *AEU-Int J Electron C*. 2021;137(April):153742. doi:10.1016/j.aeue.2021.153742
15. Yucehan T, Yuce E. A new grounded capacitance multiplier using a single ICFOA and a grounded capacitor. *IEEE Trans Circuits Syst II: Express Briefs*. 2022;69(3):729-733. doi:10.1109/TCSII.2021.3102118
16. Al-Absi MA, Abuelma'atti MT. A novel tunable grounded positive and negative impedance multiplier. *IEEE Trans Circuits Syst II: Express Briefs*. 2019;66(6):924-927. doi:10.1109/TCSII.2018.2874511
17. Özer E, Başak ME, Kaçar F. Realizations of lossy and lossless capacitance multiplier using CFOAs. *AEU-Int J Electron C*. 2020;127-(August):153444. doi:10.1016/j.aeue.2020.153444
18. Analog Devices. *AD844-60 MHz, 2000 V/μs, Monolithic Op Amp with Quad Low Noise*; 2000:20.
19. Ochoa A. *Feedback in Analog Circuits*. Springer Professional; 2016. doi:10.1007/978-3-319-26252-9
20. Leung KN, Mok KT. Analyisis of multistage amplifier-frequency compensation. *IEEE Trans Circuits Syst I: Fund Theory Appl*. 2001; 48(9):1041-1056. doi:10.1109/81.948432

How to cite this article: Beloso-Legarra J, De La Cruz-Blas CA, Carlosena A, Martincorena-Arraiza M. Very-low frequency capacitively coupled AC amplifier with a current feedback operational amplifier. *Int J Circ Theor Appl*. 2023;1-14. doi:10.1002/cta.3620